Annals of Botany **112**: 1141–1148, 2013
doi:10.1093/aob/mct172, available online at www.aob.oxfordjournals.org

ANNALS OF BOTANY
Founded 1887

Silica nanoparticles aid in structural leaf coloration in the Malaysian tropical rainforest understorey herb *Mapania caudata*

Greg Strout[1], Scott D. Russell[1,2], Drew P. Pulsifer[3], Sema Erten[3], Akhlesh Lakhtakia[3] and David W. Lee[4,*]

[1]*Samuel Roberts Noble Electron Microscopy Laboratory, University of Oklahoma, Norman, OK 73019, USA,* [2]*Department of Microbiology and Plant Biology, University of Oklahoma, Norman, OK 73019, USA,* [3]*Department of Engineering Science and Mechanics, Pennsylvania State University, University Park, PA 16802, USA and* [4]*Department of Biological Sciences, Florida International University, Miami, FL 33199, USA*
** For correspondence. E-mail leed@fiu.edu*

Received: 30 March 2013 Returned for revision: 14 May 2013 Accepted: 11 June 2013 Published electronically: 19 August 2013

• *Background and Aims* Blue-green iridescence in the tropical rainforest understorey sedge *Mapania caudata* creates structural coloration in its leaves through a novel photonic mechanism. Known structures in plants producing iridescent blues consist of altered cellulose layering within cell walls and in special bodies, and thylakoid membranes in specialized plastids. This study was undertaken in order to determine the origin of leaf iridescence in this plant with particular attention to nano-scale components contributing to this coloration.
• *Methods* Adaxial walls of leaf epidermal cells were characterized using high-pressure-frozen freeze-substituted specimens, which retain their native dimensions during observations using transmission and scanning microscopy, accompanied by energy-dispersive X-ray spectroscopy to identify the role of biogenic silica in wall-based iridescence. Biogenic silica was experimentally removed using aqueous Na_2CO_3 and optical properties were compared using spectral reflectance.
• *Key Results and Conclusions* Blue iridescence is produced in the adaxial epidermal cell wall, which contains helicoid lamellae. The blue iridescence from cell surfaces is left-circularly polarized. The position of the silica granules is entrained by the helicoid microfibrillar layers, and granules accumulate at a uniform position within the helicoids, contributing to the structure that produces the blue iridescence, as part of the unit cell responsible for 2 ° Bragg scatter. Removal of silica from the walls eliminated the blue colour. Addition of silica nanoparticles on existing cellulosic lamellae is a novel mechanism for adding structural colour in organisms.

Key words: *Mapania*, Cyperaceae, leaf, epidermis, cell wall, silica, helicoids, nanoparticle, iridescence, circular polarization, photonics.

INTRODUCTION

Advances in the fields of photonics and nanostructures have stimulated research on structural coloration in organisms, particularly in animals. The latter research has suggested the possibility of biological structures being templates for the production of new optical devices, through 'biomimetics and bioinspiration' (Martín-Palma and Lakhtakia, 2009; Bar-Cohen, 2011). Structural colour originated early in the history of multicellular organisms and has evolved in a great diversity of them (Parker, 1998; McNamara *et al.*, 2011). Research in biological structural colour goes back centuries, and the resurgence of this research in recent years has revealed an amazing variety of mechanisms for colour production, including classical thin-film interference, diffraction, photonic crystals and cholesteric liquid crystals (Kinoshita and Yokiosha, 2005). The newly discovered mechanisms are increasingly bizarre and interesting (Saranathan *et al.*, 2010). These results are from a rather narrow systematic sampling of organisms, so we can expect a continuing flow of interesting research in the area of structural colour as more organisms are examined.

Plants are less well studied than animals for structural coloration, or iridescence; perhaps the greater biochemical repertoire of plants reduces the diversity of structures in producing colours. For instance, virtually all blue and green coloration in animals is structural (Bagnara *et al.*, 2007), whereas in flowers and fruits of plants blues are commonly produced by modified anthocyanins (Lee, 2007). Nonetheless, structural coloration in plants has been analysed, e.g. in the blue leaves of tropical understorey plants, in a few tropical fruits and recently in the diffractive petal colours of a variety of flowers (Lee, 2007; Whitney *et al.*, 2009*a*; Glover and Whitney, 2010). In leaves and fruits, the physical mechanism for blue iridescence is multi-layer interference. In leaves, constructive interference is due to the higher refractive indices of cellulose in cell walls and in the thylakoid lamellae of plastids (Graham *et al.*, 1993; Gould and Lee, 1996). In fruits, multi-layered cellulosic structures are produced outside the epidermal lamella but inside the cell wall (Lee, 1991; Lee *et al.*, 2000). Recently discovered diffractive coloration (Whitney *et al.*, 2009*a*) is caused by gratings (closely packed ridges) in patches on petal surfaces, and it may be widespread (Whitney *et al.*, 2009*b*). Although few taxa have been analysed, many putatively iridescent plants await study (McPherson, 2010) and may reveal novel mechanisms of colour production (Gebeshuber and Lee, 2012).

Plants with blue iridescent leaves are most common and diverse in the shade of tropical Asian rainforests, particularly in the Malayan Peninsula (Lee, 2001). In this article we report

© The Author 2013. Published by Oxford University Press on behalf of the Annals of Botany Company. All rights reserved.
For Permissions, please email: journals.permissions@oup.com

on the ultrastructural basis for the vivid iridescent blue–green leaf coloration in a Malaysian understorey herb, *Mapania caudata* (Cyperaceae; Simpson, 1992; Fig. 1A, B), in a genus of tropical understorey herbs. Here we show that the basis for colour is the combination of helicoid cellulose deposition and the layering of silica nanoparticles in the adaxial epidermal cell wall. Such cells produce a brilliant blue which, combined with the normal chlorophyllous leaf tissue, produces a blue–green leaf.

MATERIALS AND METHODS

Plants of *Mapania caudata* for this research were provided by Dr Saw Leng Guan of the nursery of the Forest Research Institute of Malaysia, Kuala Lumpur, from individuals collected by institute personnel from the Hulu Terengannu Forest Reserve, Trengannu State, West Malaysia (FRIM herbarium no. 20040735). This species is locally common in shady, moist microclimates in forests throughout the peninsula, but particularly on the east side. Small propagules were multiplied in the Biological Science Greenhouse at Florida International University (FIU). Plants established in the simulated rainforest shade environment of the Wertheim Conservatory at FIU, as well as an adjacent greenhouse, provided the leaves used for research in this project.

Young plants were observed for growth responses (and the degree of blue–green iridescence) under different light conditions. Leaves were also examined macroscopically with a dissecting microscope and for gross anatomy using hand sections (~50 μm) and a compound light microscope.

Electron microscopy

For scanning electron microscopy (SEM), freshly collected iridescent blue leaves were cut into 1 mm squares, fixed in 2 % glutaraldehyde, 2 % paraformaldehyde in 0·1 M cacodylate buffer (pH 7·2) at 20 °C for 2 h, fixed for 2 h in 1 % OsO_4 in cacodylate buffer at 4 °C, dehydrated in an ethanol series, and critical-point dried using a Tousimis Auto Samdri CPD (Tousimis Inc., Rockville, MD). Samples were observed with a JEOL 880 scanning electron microscope operated at 15 kV (JEOL Ltd., Tokyo, Japan). For transmission electron microscopy (TEM), we fixed material using the methods described above for SEM procedures. For more precise measurements of cell wall structures we used a high-pressure freezing technique with leaf discs (2 mm in diameter) punched from blue–green iridescent leaves. Frozen leaf discs were then incubated with or without 1 % OsO_4 in distilled acetone for 20 days at −90 °C and processed according to techniques described in Fields *et al.* (1997). Samples were slowly warmed to −25 °C, transferred to 4 °C and then to room temperature, rinsed in distilled acetone and rehydrated to 100 % water in a graded series. The OsO_4-treated leaf discs were re-fixed in 1 % aqueous osmium tetroxide for 2 h. Specimens dehydrated in an ethanol series were infiltrated and embedded in Spurr's epoxy resin (Electron Microscopy Sciences, Hatfield, PA). Samples retained iridescence after specimen preparation and were used for critical observations of lamellar thickness and elemental composition (Supplementary Data Fig. S1). For TEM, samples were sectioned transversely at ~75 nm using a Reichert Ultracut E equipped with a diamond knife. Sections were retrieved and stained using aqueous uranyl acetate and Sato's lead, and photographed in a JEOL 2000FX transmission electron microscope operated at 200 kV.

Elemental analysis

Energy-dispersive X-ray analysis (EDXA) was employed to detect the presence and distribution of various elements in the leaf epidermal cells. We employed a Kevex conventional X-ray detector (Thermo Scientific, Scotts Valley, CA) equipped with IXRF Analysis Software (IXRF Systems, Austin, TX) to calculate element concentrations on the JEOL 880 at 15 kV, and an INCA system with a thin window detector (Oxford Instruments, Oxford, UK) on a JEOL 2010F scanning transmission electron microscope (STEM) equipped with a field emission gun to image the distribution of silica at 200 kV. Detectors simultaneously image energy spectra corresponding to the most abundant elements of silica, silicon (Si) and oxygen (O). Detector output was analysed using a semi-quantitative algorithm. It was assumed that the specimens constituted a flat surface with homogeneous distribution of elements in the sample, that the beam was absorbed in the 6 μm of normal wall thickness, and that the detector-to-sample geometry was normal, yielding estimates that should be correct within 10 %.

Optical analysis

Diffuse reflectance of leaf samples was measured with an Li-1800 spectroradiometer (Li-Cor Inc., Lincoln, NE) with a fibre-optic connection to an integrating sphere and containing barium sulphate as an optical white reference (Graham *et al.*, 1993), over a wavelength range of 350–850 nm. For the higher-volume analyses required by silica removal experiments, we measured surface reflectance at a fixed 90 ° angle with a Unispec-SC spectrometer (PP systems, Amesbury, MA), equipped with a fibre-optic probe inserted in the camera attachment tube of an Olympus CH compound light microscope, which provided a sample area of ~0·8 mm diameter in a wavelength range of 400–850 nm. Tungsten–halogen illumination at 45 ° was provided on both sides of the leaf sample using fibre-optic light guides, and the diffuse white reflectance card provided by the instrument manufacturer was used as a reference.

These leaves were also examined for linear and circular polarization at ×40 magnification with a dissecting microscope. For circular polarization, left and right circular polarization (LCP and RCP) filters were employed (Real-D, Beverley Hills, CA), plus a Hoya multi-coated glass X1 green filter. Because two different conventions are used to define the handedness of circularly polarized light (Lakhtakia, 1994), a well-characterized optical setup (Swiontek *et al.*, 2013) was used to ascertain whether a particular filter transmitted LCP or RCP light in the visible spectrum. Then, either an LCP or an RCP filter was placed between the sample and objective lenses of the microscope to detect either LCP or RCP light reflected from the leaf surface.

Silica removal

To determine the role of silica in producing blue-enriched iridescence, it was necessary to develop methods of removal and to measure changes in optical properties correlated with their

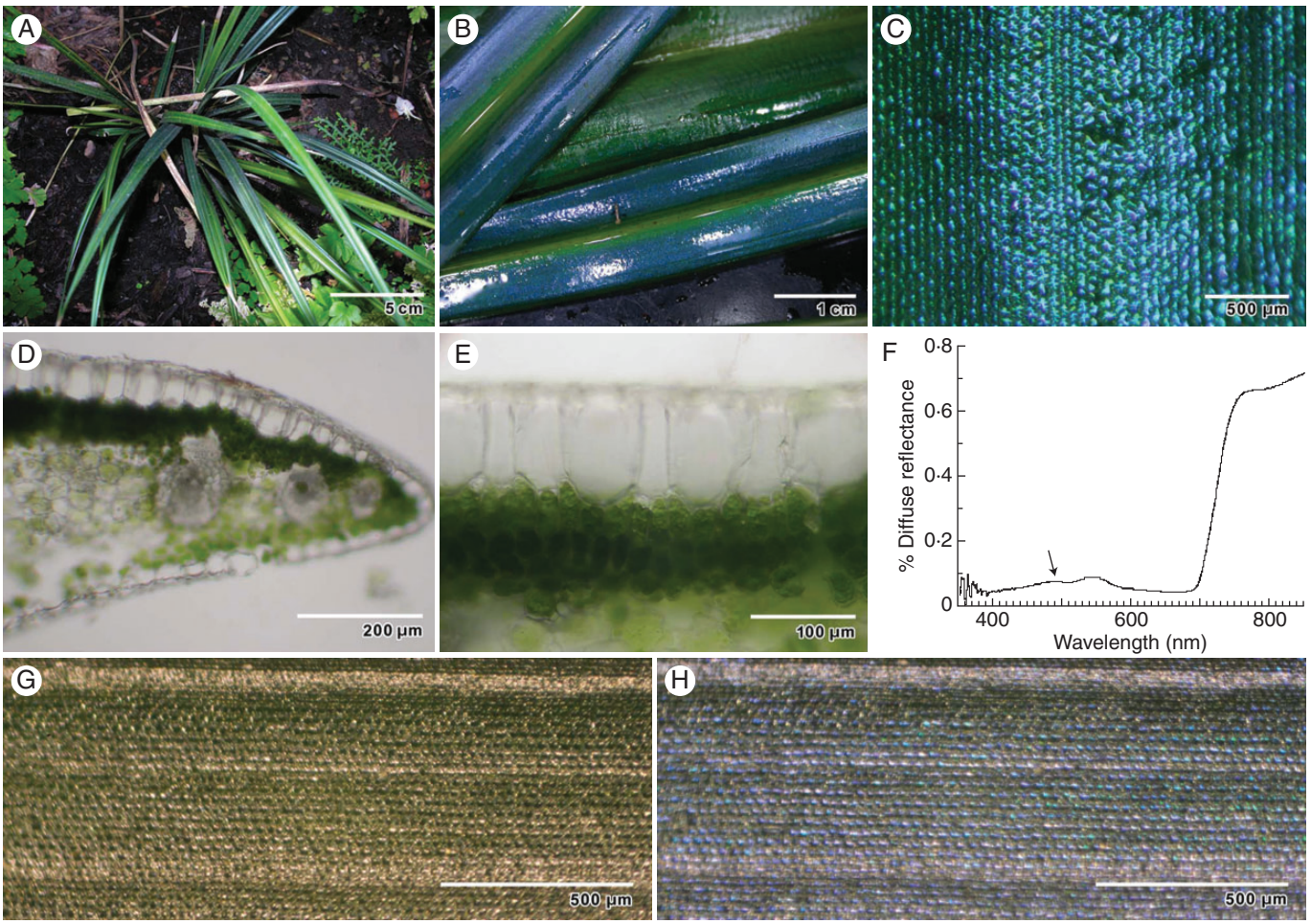

FIG. 1. General appearance of *M. caudata* leaf structure by light microscopy, and optical properties. (A) Young plants growing in shade. (B) Intense blue–green iridescent colour from edge of leaf to midrib. (C) Reflected light on the surface of the leaf reveals iridescence of individual epidermal cells. (D) Transverse section of freshly sectioned leaf showing dense chloroplast concentration in palisade mesophyll, and rhomboidal epidermal cells. (E) Transverse section of epidermal cells shows thickened adaxial cell wall. (F) Diffuse spectral reflectance of typical iridescent blue leaf. Arrow indicates blue peak. (G) Leaf surface reflectance observed with a right circularly polarizing (RCP) filter. (H) Leaf surface reflectance observed with corresponding LCP filter.

concentration. Initially we treated leaf samples with 10 % HF for 15 min for indiscriminate removal of Si, and we found a significant reduction in both silica and iridescence (Strout *et al.*, 1999). Additional experiments with HF (10 % and 20 min) and HCl controls (24 % and 20 min, equivalent to HF in normality) revealed extensive tissue alterations by both treatments along with loss of iridescence, although there was slight residual iridescence after the HCl treatment. The HF procedure, being unselective in Si removal and visibly damaging to the tissue, was supplemented by a less destructive treatment using solutions of 2 % anhydrous Na_2CO_3 in dH_2O (0·07 M), which selectively removes biogenic Si (Saccone *et al.*, 2006, 2007). We tested the solution for refractive index (η) with a refractometer. After partial evacuation five times to facilitate solution movement into 4 × 4 mm leaf squares, samples were incubated at 23 °C for 24 h; control samples were incubated in H_2O. We performed the same extraction on blue leaves of *Elaphoglossum metallicum*, obtained from the Atlanta Botanical Garden. Treated leaves of *M. caudata* retained their green colour, with intact chloroplasts. We also removed the Na_2CO_3 from these leaves by replacement with dH_2O to test for any change in colour. Leaf samples were assessed for surface reflectance before and after treatment, ensuring that all samples were similar in degree of blue–green iridescent colour and providing an evaluation of treatment effects. Samples were then fixed in 2 ml of 3 % glutaraldehyde at pH 7·0 in 0·05 M phosphate buffer for 24 h at 3 °C. Samples were washed twice in distilled H_2O and then dehydrated in four steps to 60 % ethanol. Samples were then measured for silica concentration and distribution using EDXA and STEM.

Statistical analysis

We sampled leaf tissue from four individual plants derived from offshoots of two individuals. For microscopic analysis of cell wall structures, we sampled 30 sections, an average of three to four transects per section per statistical dataset. For experiments to remove silica from leaves, we examined five leaves from each treatment, with three optical measurements of each leaf before and after treatment. Each of these leaves was

then measured for silica content and distribution. Differences between treatments were compared by one-tailed *t*-tests.

RESULTS

Examination of leaf samples indicated that leaves varied in intensity of iridescence, but all leaves were iridescent to some degree (Fig. 1A–C). Blue–green iridescence was enhanced in leaves of plants grown under deep shade in the conservatory compared with plants grown under ~30 % sunlight in the greenhouse. When the blue–green leaves were partially desiccated the blue vanished, but it was partially restored by rehydration. These leaves had two diffuse reflectance peaks, one in the green region (at ~550 nm wavelength) and one in the blue region (489 ± 9 nm, $n = 5$; Fig. 1F) of the visible spectrum. Macroscopic observations of blue–green leaf iridescence revealed continuous areas of blue colour originating from individual tiled epidermal cells. Microscopic observations of the leaf surface indicated that colour production (the sharpest resolution of colour) originated from the adaxial walls of epidermal cells (Fig. 1C). These walls were 6·4 ± 0·5 (s.e.) μm thick ($n = 5$), as measured in transverse sections (Fig. 1D, E and 2A).

Light reflected from the cell surface was plane-polarized. When a linear polarizer inserted between the leaf surface and the experimenter's eyes was rotated about an axis normal to the polarizer, no discernible changes were seen. When the combination of a green filter and either a left circular polarization (LCP) or a right circular polarization (RCP) filter was superposed between the leaf surface and the experimenter's eyes, the circular polarization filter had no effect, indicating that green light reflected from the leaf surface did not have a preferential polarization. However, when the green filter was removed, blue light reflected from the leaf surface was predominately left-circularly polarized. Further examination of the blue light with the experimenter's eyes replaced by a ×40 dissecting microscope clearly indicated that most cells on the leaf surface were responsible for the LCP blue colour (Fig. 1G, H).

Details in the structure of the cell wall were revealed by electron microscopy. In SEM, a transverse razor-blade cut through the wall showed alternating layers based on tissue orientation relative to the cut, thus apparently either projecting or receding with respect to the epidermal surface (Fig. 2B). In TEM, these appeared as two periodic features of the wall. The first was the loose helicoid appearance of the wall microfibrils, which alternated with darker groupings of microfibrils where layers intersected (Fig. 2C, E). Multiple layers (32 ± 2, $n = 4$) were seen in all leaves. Individual layer thickness was estimated by dividing the total thickness of layering by the number of layers in 1 μm midway across the wall; it was 167 ± 2 nm. The electron-opaque layers consisted of granules of irregular structure, varying from 15 to 45 nm in diameter. The granules themselves were not uniform in appearance, containing numerous areas that were more electron-opaque than others. Layers with granules were most pronounced near the adaxial surface and midway through the adaxial wall (Fig. 2D). Epidermal walls of cells from regions of leaves with no blue iridescence lacked the granules but retained the helicoid appearance (Fig. 2F, Supplementary Data Fig. S?).

Analysis of the cell wall by EDXA revealed the Si and O elemental signatures of silica in areas that corresponded to the electron-opaque granules (Fig. 3A–C). Peaks of silica (Si + O) corresponded with these electron-dense granules in transects of the cell wall, as well as in the semi-quantitative scans superimposing EDXA quantitative images corresponding to Si and O on the TEM images (Fig. 3B, C). Tissue extraction with aqueous Na_2CO_3 ($\eta = 1{\cdot}37$) was effective in removing silica from the leaf tissue samples. Whereas iridescent blue–green control leaves had relatively high concentrations of silica, green-coloured Na_2CO_3-extracted leaves had low, essentially non-detectable, amounts of Si, as indicated by TEM and EDXA (Fig. 3F). When Na_2CO_3 was removed from the leaf samples, the green colour did not change. These leaves were also depleted in electron-opaque granules (Fig. 3F), and their corresponding spectrographic plots confirmed the loss of the blue iridescent peak from the extracted tissue (Fig. 3D, E). The degree of iridescence was determined for each specimen by the difference in surface reflectance at low reflectance (506 nm) and at maximum blue reflectance (463 nm). The blue reflectance peak was approximately the same height as the green chlorophyll reflectance peak, and it was significantly higher than that in the Na_2CO_3-treated leaves ($P < 0{\cdot}005$). In *E. metallicum*, Na_2Co_3 treatments did not alter the blue leaf colour. Use of HF also removed Si from treated leaves of *M. caudata* (Supplementary Data Fig. S3) and in addition appeared to remove green iridescence in white- and blue-enriched incident light range.

DISCUSSION

The results of this research are consistent with the role of a novel material (for plants, at least) in structural colour: silica. In previous research on plant iridescence the structural basis has been found to consist of lamellae composed of cellulose. In *Selaginella*, the few layers consisting of cellulose occur as electron-opaque regions alternating with lighter non-cellulosic layers (Hébant and Lee, 1984; Thomas *et al.*, 2010). In the fruits of *Elaeocarpus angustifolius* (Lee, 1991) and *Delarbrea michieana* (Lee *et al.*, 2000), the complex layering of cellulosic structures, secreted by the epidermal cells but within the cell wall, accounts for the brilliant blue iridescence. In ferns of the Asian tropics (Gould and Lee, 1996) and neotropics (Graham *et al.*, 1993), cellulose microfibrils are laid down at a constantly differing angle from previous depositions, producing a helicoid morphology (Neville and Levy, 1985; Kutschera, 2008) like that of a cholesteric liquid crystal (Collings, 1990) or a chiral sculptured thin film (Lakhtakia and Messier, 2005). The helicoid morphology produces iridescence that can be appreciated in the visible spectrum. This iridescence can be viewed with circularly polarized light of the same handedness as the helicoid morphology, but not with circularly polarized light of the other handedness, similar to some beetle exocuticles with structural chirality (Neville and Caveney, 1969). Discrimination of the circular polarization state of incident light is absent when the sequence of depositions does not have a helicoid nature but instead the refractive index varies periodically. As examples, multiple thylakoid membranes of predicted thicknesses account for iridescence in a neotropical fern, *Trichomanes elegans* (Graham *et al.*, 1993), as well as Asian iridescent begonias and two species of *Phyllagathis* (Gould and Lee, 1996).

Two partially overlapping periodicities in the epidermal cell wall structure in *Mapania caudata* might account for the blue

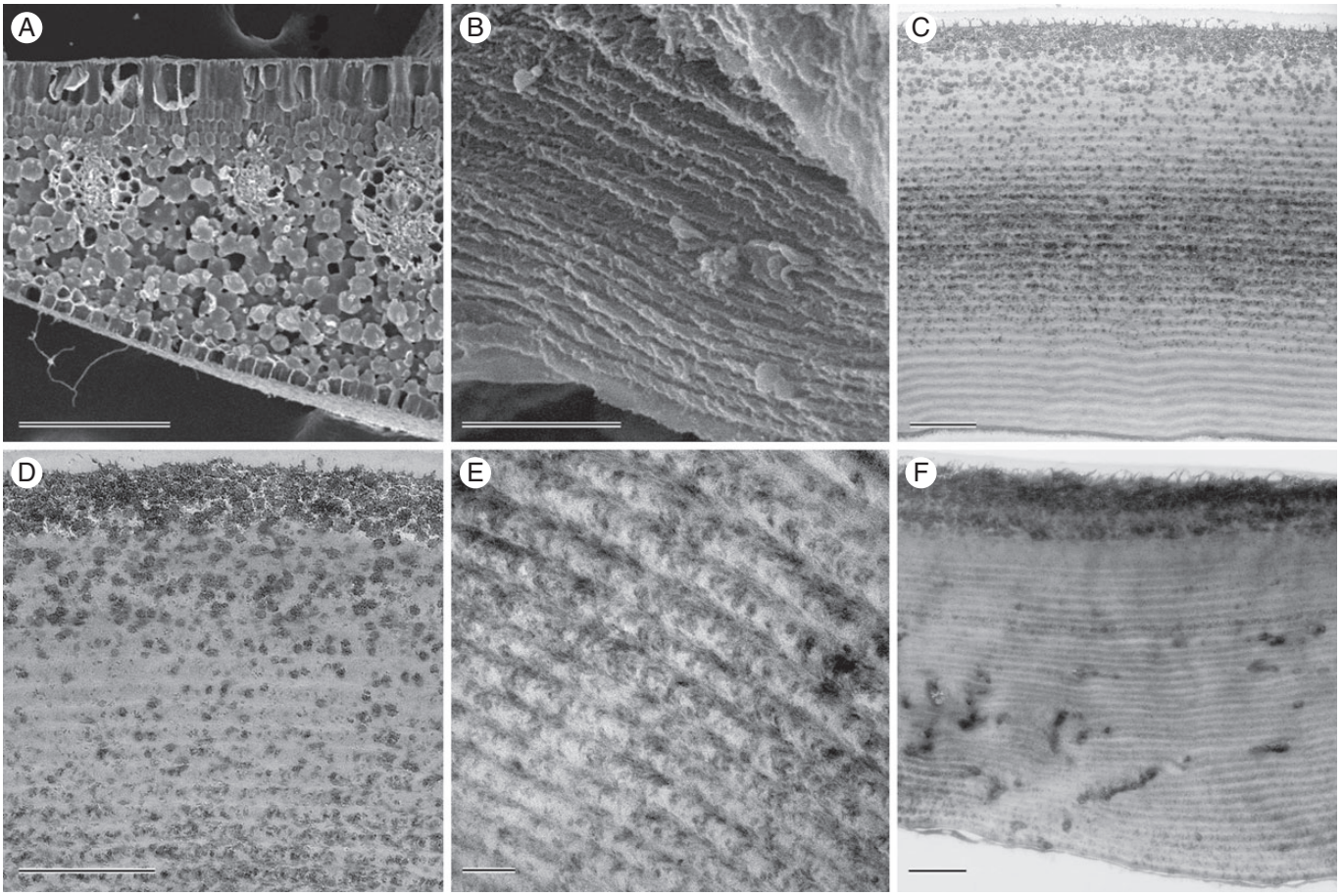

FIG. 2. Electron microscopy of leaves of *M. caudata*. (A) SEM of leaf transverse section showing rhomboidal epidermal cells and densely packed palisade mesophyll cells. (B) Adaxial epidermal cell in SEM, revealing wall layering present through most of the width of the wall. (C) TEM of transverse adaxial epidermal cell wall shows layers of alternating electron translucency and a thicker, single granular layer near the surface. (D) Higher magnification TEM image near adaxial surface showing relationship of granules and helicoid layering. (E) TEM of adaxial wall near the middle of the adaxial wall, revealing helicoid appearance in finer detail. (F) TEM of adaxial epidermal cell wall in a non-iridescent portion of the leaf. Scale bars: (A) = 200 μm; (B–F) = 1 μm.

structural coloration. The first is the helicoid layering of cellulose microfibrils, which remains highly uniform throughout the epidermal cell walls. The second is the aggregation of silica nanoparticles, which are associated with a sector of the helicoids that appears to be able to entrain their positioning. How do they account for the colour production?

Details in the structure of the cell wall were revealed by electron microscopy using high-pressure freezing and freeze substitution to maintain lamellar dimensions at their native distance, accompanied by chemical extraction and observation of living material (Supplementary Data Fig. S1C). Together, these data yield clues in explaining the production of blue colour, at a peak wavelength of 489 nm. In SEM, a transverse razor-blade cut through the wall showed alternating layers of projecting and receding tissues (Fig. 2B). In TEM these appeared as two periodic features of the wall. The first was a loose helicoid arrangement, with thick, loosely arranged 'strands' (Fig. 2C, E). The second was a periodicity in rough granular, electron-opaque particles associated with the helicoid layering (Fig. 2C, D). Multiple layers (32 ± 2, $n = 4$, ~100 nm thick) were seen in all leaves. Each helicoid strand had a pitch ($p = 334$ nm). Each half of the assembly of helical strands (of thickness 167 nm) comprised a silica-rich layer and a silica-poor layer. The silica-poor layer was primarily cellulosic, while the silica-rich layer contained a large volume fraction of silica granules with cross-sectional radius in the 15–45 nm range, along with cellulose.

To determine whether the helicoid strands are sufficient by themselves to produce the blue iridescence, we calculated the refractive index required to produce the measured wavelength peak at the periodicity and lamellar spacings measured using high-pressure frozen, freeze-substituted TEM samples. Thus, we were able to calculate the average refractive index (η_{avg}) of the lamellar distance. For the blue colour to come from the helicoid strands requires that $\eta_{avg} = 489\ \text{nm}/p = 1{\cdot}464$. If, however, the blue colour does not come from the helicoid strands but simply from a dielectric mirror formed by alternating silica-rich and silica-poor layers, both of which are macroscopically homogeneous, then $\eta_{avg} = 489\ \text{nm}/(2p/2) = 1{\cdot}464$. Therefore, examination with circular-polarization filters is necessary in order to distinguish between the two possible mechanisms for the production of blue structural colour.

The production of blue colour turned out to be associated with left circular polarization. The difference in colour between

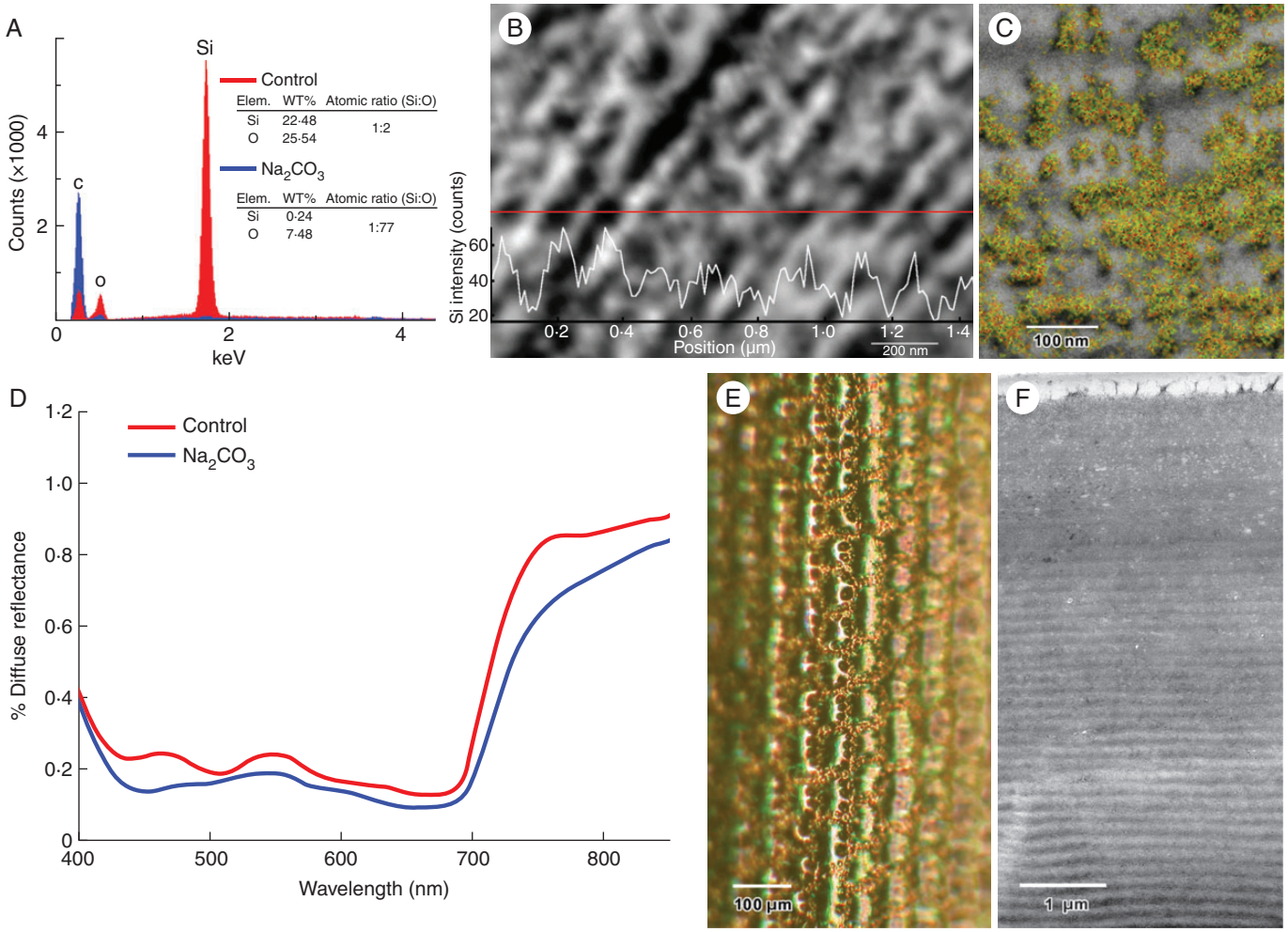

FIG. 3. Detection, distribution and removal of silica from adaxial epidermal cell walls. (A) Energy dispersive X-ray spectra of electron-opaque granular particles near the adaxial surface (red) versus control (blue) reveal strong signal peaks for silicon and oxygen in granular region corresponding with the presence of silica (SiO_2). The approximate ratio of 2:1 is consistent with the presence of SiO_2. (B) EDXA line scans transecting particle-decorated microfibrillar lamellar regions indicate Si energy-related peaks correlate closely with electron opaque granular bodies. (C) Semi-quantitative EDXA map combining the red silicon $K\alpha_1$ peak values with the green oxygen $K\alpha 1$ peak values. Electron-opaque granules in this scanning transmission electron micrograph correlate closely with the yellow label of the SiO_2 signal. (D) Surface reflectance of Na_2CO_3-treated leaves (blue line) indicates preferential depletion of biogenic silica near the blue peak compared with control treatments (red line). Reflectance is based on mean of three scans for each treatment ($n = 5$ leaves). (E) Leaf treated with Na_2CO_3 displays loss of iridescence with depletion of biogenic silica. (F) TEM image confirms loss of electron-opaque silica inclusions from adaxial cell walls after incubation of leaf in Na_2CO_3 (cf. Fig. 2C).

panels G and H in Fig. 3 indicates that light reflected from the leaves is primarily left-circularly polarized in the blue region of the spectrum and that the blue colour is due to the circular Bragg phenomenon (Lakhtakia and Messier, 2005). Since the leaves do not have a mottled appearance under circular polarization filters when viewed with the naked eye, a preponderance of the surface cells have similar optical characteristics. Overall, there is more uniform structure and less intense colour production than in the fruits of *Pollia condensata* (Vignolini *et al.* 2012).

The functional role of silica in the structural production of blue–green colour in *M. caudata* is supported by the experimental removal of silica from the cell wall by extraction with Na_2CO_3, which removes biogenic silica depositions (Saccone *et al.*, 2006). The success of the Na_2CO_3 incubation procedure was verified by both the low amount of Si detected afterwards by EDXA analysis, and also by the lack of silica granules in transverse sections seen in TEM (Fig. 3F). The Na_2CO_3 solution was slightly increased in refractive index ($\eta = 1{\cdot}37$), but this was not enough to affect the function of the colour-producing structures. Furthermore, removal of the Na_2CO_3 after treatment did not revert the colour produced to blue. TEM imaging of an exterior cell wall lacking iridescence revealed the helicoid wall structure, and electron-opaque granular layers were absent (Fig. 2F). The silica nanoparticles formed discrete multi-layers (~32 of them, roughly 100 nm in thickness) that can account for such colour production (Fig. 2B–D). Silica has a refractive index of 1·475 (Khlebtsov *et al.* 2008), different from that of cellulose in the cell walls ($\eta = 1{\cdot}415$ when fully hydrated and higher when dried, $\eta = 1{\cdot}530$; Woolley, 1975). The loose arrangement of cellulose in the wall is likely to depress the refractive index of cellulose in the wall from the fully hydrated value. Rapid dehydration of leaf samples (which would increase the refractive

index of cellulose) removed the blue iridescence, which was partially restored by rehydration. Chemically bound water removed by desiccation is presumably not restored by rehydration and therefore does not fully restore the wall's native structural configuration. Although the Na_2CO_3 incubation did not remove iridescent blue from another plant, *E. metallicum* (with left-circular polarization and, presumably, helicoid walls), it is still possible that the treatment could alter wall properties and iridescence in some unknown way.

Peak reflectance at 489 nm wavelength requires that the average refractive index should be 1·464, which suggests that the cellulose is partially hydrated, with a refractive index of $>1{\cdot}415$, probably 1·46 (Woolley, 1975); this differs from that of silica alone. If the silica granules were to be replaced by air ($\eta = 1$), the effective refractive index of the originally silica-rich layer in the unit cell would drop precipitously, thereby lowering the average refractive index to a value of $<1{\cdot}2$; consequently, the peak reflectance characteristic of a dielectric mirror would slip into the ultraviolet regime and be invisible to humans. Even if the silica granules were to be replaced by water ($\eta = 1{\cdot}33$), the average refractive index would still be lowered and the reflectance peak would shift considerably towards 400 nm. If the silica granules were left intact but the leaf were dried, the average refractive index would increase significantly because the refractive index of dry cellulose is significantly higher than that of silica, moving the peak reflectance into the green part of the visible spectrum.

The reflectance peaks in Fig. 1F are quite broad. The thickness of layers can vary considerably in each leaf, which is responsible for the broadening. This phenomenon is seen most vividly in silver fish skins (McKenzie *et al.*, 1995).

It will be interesting to look for this mechanism in other plants that sequester silica in cell walls. The presence of silica in plants is phylogenetically constrained (Hodson *et al.*, 2005), and widespread in the order Poales. Since the presence of silica adds to fitness in rice and cucumbers, among other plants, we have learned much about the mechanisms of Si uptake (Raven, 2003; Ma and Yamaji, 2006) and the particular importance of silica in aquatic macrophytes (Schoelynck *et al.*, 2010). The most extensive survey of documented iridescence (McPherson, 2010) included a second species of *Mapania* (*M. meditensis*) from Thailand, an orchid (*Aspidogyne costaricensis*), a palm (*Chamaeodorea metallica*), but no grasses. A broader and more speculative survey (Gebeshuber and Lee, 2012) suggested analysing both grasses and sedges. Inflorescences of the grasses *Miscanthus sinensis* and *Pennisetum alopecuroides* are iridescent. Among the sedges, *Mapania graminea* may also have blue iridescent leaves, and leaves within *Carex* (*C. dipsacea*, *C. flagellifera* and *C. squarrosa*) are iridescent blue–green. Seedlings of *Fimbristylis* may also be iridescent (*F. annua*, *F. vahlii* and *F. perpusilla*). These would be good candidate species in which to examine the role of silica in iridescence.

Iridescent blue leaves are characteristic of a small number of tropical rainforest plants of extreme shade. Other than *Selaginella*, with peak reflectance at 420 nm (Thomas *et al.*, 2010), all other species have peak reflectances of 448–489 nm. The similar reflectance properties and light requirements of these plants suggest a common function, but we have no satisfactory explanation to date. Lee and Lowry (1975) suggested that such layers in *Selaginella* could function as anti-reflection coatings, thus allowing greater absorption of much longer wavelengths. However, Thomas *et al.* (2010) preferred a co-evolutionary mechanism: reducing herbivory on such leaves. Another possibility is that increased reflectance of blue in iridescent leaves may protect such plants against photo-damage during brief light flecks (Lee *et al.*, 2008).

The silica structures in *M. caudata* are simpler and much less elegant than the elaborate frustules of diatoms (Fuhrmann *et al.*, 2004; Mazumder *et al.*, 2010), with hexagonal pore arrays in a lattice with photonic resonances. Yet the multiple layers make them effective in producing an iridescent blue colour. There is much interest now in using organisms such as diatoms as templates or inspirations for new photonic devices. Experiments with layer-by-layer deposition of nanoparticles that contain SiO_2 have used the principles of biological colour to produce tunable filters at a variety of wavelengths (Kurt *et al.*, 2009), and chirality has been introduced into mesoporous silica to produce novel reflective filters with selective handedness (Shopsowitz *et al.*, 2010), each of which incorporates silica nanoparticle arrays similar to those observed in *M. caudata* to produce elaborate photonic coatings. Nonetheless, this silicate structure is a novel mechanism for the production of structural colour in plants, added to the layering of cellulose in walls and the modification of plastids previously described. This mechanism may account for iridescent colours in other species of *Mapania*, a pantropical genus of some 73 species, mostly of tropical rainforest understorey plants (Simpson, 1992), and in other taxa of the Cyperaceae. Thus, structural colouring mechanisms involving silica may not be limited to *Mapania caudata.*

SUPPLEMENTARY DATA

Supplementary data are available online at www.aob.oxfordjournals.org and consist of the following. Figure S1: comparison of iridescence before and after freezing, substitution, infiltration and embedding. Figure S2: the area used to generate the EDXA spectra shown in Fig. 3A. Figure S3: results of treatments using hydrofloric acid to remove silica, along with corresponding EDXA spectra and iridescence reduction. Figure S4: illustration of light, SEM and TEM details regarding the organization of leaf cell walls in *M. caudata*.

ACKNOWLEDGEMENTS

This research was financially supported by the Department of Biological Sciences at Florida International University and by the Department of Microbiology and Plant Biology and the Vice President for Research at the University of Oklahoma (OU). D.W.L. received support from the National Geographic Society, Committee on Research and Exploration, to collect plants and tissues of *Mapania caudata*. We acknowledge excellent technical support and advice at OU by Dr Preston Larson, SRNEML; Dr Lloyd Bumm, Department of Physics and Astronomy; and Cal Lemke, Department of Microbiology and Plant Biology; and at FIU by Dr Andrew McFarland, Department of Earth and Environment. Dr Chad Husby (Montgomery Botanical Center, Miami), Mr Ron Determann and Mr Michael Wenzel (Atlanta Botanical Garden) provided plants important in later stages of the research.

LITERATURE CITED

Bagnara JT, Fernandez PJ, Fujii R. 2007. On the blue coloration of vertebrates. *Pigment Cell Research* **20**: 14–26.

Bar-Cohen Y. ed. 2011. *Biomimetics: nature-bound innovation*. Boca Raton, FL: CRC Press.

Collings PJ. 1990. *Liquid crystals: nature's delicate phase of matter*. Princeton, NJ: Princeton University Press.

Fields SD, Strout GW, Russell SD. 1997. Spray-freezing freeze substitution (SFFS) of cell suspensions for improved preservation of ultrastructure. *Microscopy Research and Technique* **38**: 315–328.

Fuhrmann T, Landwehr S, El Rharbi-Kucki M, Sumper M. 2004. Diatoms as living photonic crystals. *Applied Physics B* **78**: 257–260.

Gebeshuber IC, Lee DW. 2012. Nanostructures for coloration (plants). In: Bushan B. ed. *Encyclopedia of nanotechnology*. Heidelberg: Springer, 1790–1803.

Glover BJ, Whitney HM. 2010. Structural colour and iridescence in plants: the poorly studied relations of pigment colour. *Annals of Botany* **105**: 505–511.

Gould KS, Lee DW. 1996. Physical and ultrastructural basis of blue leaf iridescence in four Malaysian understory plants. *American Journal of Botany* **83**: 45–50.

Graham RM, Lee DW, Norstog K. 1993. Physical and ultrastructural basis of blue leaf iridescence in two neotropical ferns. *American Journal of Botany* **71**: 198–203.

Hébant C, Lee DW. 1984. Ultrastructural basis and developmental control of blue iridescence in *Selaginella* leaves. *American Journal of Botany* **71**: 216–219.

Hodson MJ, White PJ, Mead A, Broadley MR. 2005. Phylogenetic variation in the silicon composition of plants. *Annals of Botany* **96**: 1027–1046.

Khlebtsov BN, Khanadeev VA, Khlebtsov NG. 2008. Determination of the size, concentration, and refractive index of silica nanoparticles from turbidity spectra. *Langmuir* **24**: 8964–8970.

Kinoshita S, Yoshioka S. eds. 2005. *Structural colors in biological systems. Principles and applications*. Osaka: Osaka University Press.

Kurt P, Banerjee D, Shen RE, Rubner MF. 2009. Structural color via layer-by-layer depositions: layered nanoparticle arrays with near-UV and visible reflectivity bands. *Journal of Materials Chemistry* **19**: 8920–8927.

Kutschera U. 2008. The growing outer epidermal wall: design and physiological role of a composite structure. *Annals of Botany* **101**: 615–621.

Lakhtakia A. 1994. *Beltrami fields in isotropic chiral media*. Singapore: World Scientific.

Lakhtakia A, Messier R. 2005. *Sculptured thin films: nanoengineered morphology and optics*. Bellingham, WA: SPIE.

Martín-Palma RJ, Lakhtakia A. eds. 2009. *Biomimetics and bioinspiration*. Bellingham, WA: SPIE.

Lee DW. 1991. Ultrastructural basis and function of iridescent blue colour of fruits in *Elaeocarpus*. *Nature* **349**: 260–262.

Lee DW. 2001. Leaf colour in tropical plants: some progress and much mystery. In: Wong K.M. ed.: Proceedings of the Stone Memorial Symposium. *Malayan Nature Journal* **55**: 117–131.

Lee DW. 2007. *Nature's palette. The science of plant color*. Chicago: University of Chicago Press.

Lee DW, Lowry JB. 1975. Iridescent blue plants: physical basis and ecologic significance. *Nature* **254**: 50–51.

Lee DW, Taylor GT, Irvine AK. 2000. Structural fruit coloration *in Delarbrea michieana* (Araliaceae). *International Journal of Plant Science* **161**: 297–300.

Lee DW, Richards JH, Kelley JC. 2008. Blue leaf iridescence as a by-product of photoprotection in tropical rainforest understory plants. 58th BSA Meetings, Vancouver, BC, July. http://2008.botanyconference.org/engine/search/index.php?func=detail&aid=551.

Ma JF, Yamaji N. 2006. Silicon uptake and accumulation in higher plants. *Trends in Plant Science* **11**: 392–397.

Mazumder N, Gogoi A, Kalita RD, Ahmed GA, Buragohain AK, Choudhury A. 2010. Luminescence studies of fresh water diatom frustules. *Indian Journal of Physics* **84**: 665–669.

McKenzie DR, Yin Y, McFall WD. 1995. Silvery fish skin as an example of a chaotic reflector. *Proceedings of the Royal Society of London A* **451**: 579–584.

McNamara ME, Briggs DEG, Orr PJ, Noh H, Cao H. 2011. The original colours of fossil beetles. *Proceedings of the Royal Society of London B* **279**: 1114–1121.

McPherson S. 2010. Iridescent plants of the world. *Plantsman* **9**: 120–125.

Neville AC, Caveney SC. 1969. Scarabaeid beetle exocuticle as an optical analogue of a cholesteric liquid crystal. *Biological Reviews* **44**: 531–562.

Neville AC, Levy S. 1985. The helicoidal concept in plant cell wall ultrastructure and morphogenesis. In: Brett CT, Hillman JR. eds. *Biochemistry of plant cell walls*. Cambridge: Cambridge University Press, 94–124.

Parker A. 1998. Colour in Burgess shale animals and the effect of light on evolution in the Cambrian. *Proceedings of the Royal Society of London B* **265**: 967–972.

Raven JA. 2003. Cycling silicon – the role of accumulation in plants. *New Phytologist* **158**: 419–430.

Saccone L, Conley DJ, Sauer D. 2006. Methodologies for amorphous silica analysis. *Journal of Geochemical Exploration* **88**: 235–238.

Saccone L, Conley DJ, Koning E, *et al*. 2007. Assessing the extraction and quantification of amorphous silica in soils of forest and grassland ecosystems. *European Journal of Soil Science* **58**: 1446–1459.

Saranathan V, Osuj CO, Mochrie SGJ, *et al*. 2010. Structure, function, and self-assembly of single network gyroid (I4132) photonic crystals in butterfly wing scales. *Proceedings of the National Academy of Sciences, USA* **107**: 11676–11681.

Schoelynck J, Bal K, Backx HT, Okruszko TP, Meire P, Struyf E. 2010. Silica uptake in aquatic and wetland macrophytes: a strategic choice between silica, lignin and cellulose? *New Phytologist* **186**: 385–391.

Shopsowitz KE, Qi H, Hamad WY, MacLachlan MJ. 2010. Free-standing mesoporous silica films with tunable chiral nematic structures. *Nature* **468**: 422–426.

Simpson DA. 1992. *A revision of the genus* Mapania *(Cyperaceae)*. Richmond: Royal Botanical Gardens, Kew.

Strout G, Russell S, Lee DW. 2009. Ultrastructural basis for blue iridescence in a tropical Asian sedge: *Mapania caudata*. 59th BSA Meetings, Snowbird, UT, July. http://2009.botanyconference.org/engine/search/index.php?func=detail&aid=931.

Swiontek SE, Pulsifer DP, Xu J, Lakhtakia A. 2013. Suppression of circular Bragg phenomenon in chiral sculptured thin films produced with simultaneous rocking and rotation of substrate during serial bideposition. *Journal of Nanophotonics* **7**: doi:10.1117/1.JNP.7.073599.

Thomas KR, Kolle M, Whitney HM, Glover BJ, Steiner U. 2010. Function of blue iridescence in tropical understorey plants. *Journal of the Royal Society Interface* **7**: 1699–1707.

Vignolini S, Rudall PJ, Rowland AV, *et al*. 2012. Pointillist structural colour in *Pollia condensata* fruit. *Proceedings of the National Academy of Sciences, USA* **109**: 15712–15715.

Whitney HM, Kolle M, Andrew P, Chittka L, Steiner U, Glover BJ. 2009*a*. Floral iridescence, produced by diffractive optics, acts as a cue for animal pollinators. *Science* **323**: 130–133.

Whitney HM, Kolle M, Alvarez-Fernandez R, Steiner U, Glover BJ. 2009*b*. Contributions of iridescence to floral patterning. *Communicative & Integrative Biology* **2:** 230–232.

Woolley JT. 1975. Refractive index of soybean leaf cell-walls. *Plant Physiology* **55**: 172–174.